Research Square

Preprints are preliminary reports that have not undergone peer review.
They should not be considered conclusive, used to inform clinical practice,
or referenced by the media as validated information.

Data-Efficient Continuous Walking Fatigue Prediction using Kinect Stride Features

Parham Yazdani
Semnan University
Hadi Soltanizadeh
h_soltanizadeh@semnan.ac.ir
Semnan University
Farhad Azadi
University of Social Welfare and Rehabilitation Sciences
Mohammad Zahraei
Semnan University

Research Article

Keywords: Walking Fatigue, Kinect Sensor, Grey Wolf Optimizer, Fuzzy Fusion, Data-Efficient Learning, Gait Analysis

Posted Date: September 30th, 2026

DOI: https://doi.org/10.21203/rs.3.rs-11061494/v1

License: This work is licensed under a Creative Commons Attribution 4.0 International License.
Read Full License

Additional Declarations: No competing interests reported.

Data-Efficient Continuous Walking Fatigue Prediction using Kinect Stride Features

Parham Yazdani, Department of Electrical and Computer Engineering, Semnan University, Semnan, Iran.parhamyazdani@semnan.ac.ir
ORCID: 0009-0004-7642-2215

Hadi Soltanizadeh*, Department of Electrical and Computer Engineering, Semnan University, Semnan, Iran. h_soltanizadeh@semnan.ac.ir
ORCID: 0000-0002-2210-675X

Farhad Azadi, University of Social Welfare and Rehabilitation Sciences, Tehran, Iran.fa.azadi@uswr.ac.ir

Mohammad Zahraei, Department of Electrical and Computer Engineering , Semnan University, Semnan, Iran.mhdzahrayee@yahoo.com

***Corresponding author:** Hadi Soltanizadeh, Department of Electrical and Computer Engineering, Semnan University, Semnan, Iran. h_soltanizadeh@semnan.ac.ir

Abstract

Background & Objective: Continuous monitoring of walking fatigue is essential for clinical rehabilitation and occupational safety, yet traditional methods are often invasive or rely on large-scale datasets for deep learning, which are scarce in biomechanics. This study aims to develop a data-efficient framework for predicting continuous fatigue trajectories in unseen individuals by leveraging a database of physiologically anchored features and optimized coefficients.
Methods: We pooled data from 42 healthy adults walking to fatigue. Eight optimum Kinect-derived stride features were identified using the Grey Wolf Optimizer (GWO) and anchored to Borg RPE and sEMG. We proposed a predictive pipeline that uses a 200-second initial gait signature to identify similar individuals in a database. Three transfer learning strategies—Nearest Person, K-Nearest Neighbors (KNN), and a novel Fuzzy Fusion—were evaluated under a leave-one-subject-out (LOSO) protocol and validated on three external participants.
Results: The 200-second gait signature achieved 100% identification accuracy (Cohen's $d = 3.22$, $p < 0.0001$). In LOSO cross-validation, the Fuzzy Fusion method significantly outperformed other strategies, achieving a mean Fidelity Score of 90.88% (MAE = 9.12%). External validation on unseen participants confirmed these results, with Fuzzy Fusion maintaining a high Fidelity Score of 89.39%, reducing error by up to 49.15% compared to the Nearest Person approach.
Conclusions: The proposed GWO-anchored Fuzzy Fusion framework provides a robust, data-efficient solution for continuous fatigue monitoring. By utilizing a brief initial observation to unlock personalized predictive models, this approach circumvents the data bottleneck of deep learning and offers a practical route for low-cost, real-time physiological assessment.

Keywords: Walking Fatigue; Kinect Sensor; Grey Wolf Optimizer; Fuzzy Fusion; Data-Efficient Learning; Gait Analysis.

1. Introduction

Human walking fatigue is a complex physiological phenomenon that significantly impacts gait kinematics, increases the risk of falls, and reduces overall physical performance [1–3]. Accurate and continuous monitoring of fatigue progression is crucial for various applications, including rehabilitation, sports science, and occupational safety [4–7]. Traditional methods for assessing fatigue often rely on subjective self-reports, such as the Borg Rating of Perceived Exertion (RPE) [8–11], or invasive physiological measurements like electromyography (sEMG) [12–14]. While these methods provide valuable insights, they are often discontinuous, labor-intensive, and not suitable for real-time, low-cost, and unobtrusive monitoring in ecological settings [15–18]. Furthermore, subjective measures are inherently susceptible to inter-individual variability in perception, while invasive methods impose practical constraints that limit their deployment in everyday or field-based scenarios. This highlights a critical need for objective, continuous, and accessible methods for fatigue assessment.

Recent advancements in sensor technology, particularly markerless motion capture systems like Microsoft Kinect, have opened new avenues for gait analysis. The Kinect sensor, with its ability to capture 3D joint positions without requiring body-worn markers, offers a cost-effective and user-friendly solution for biomechanical assessment [19–21]. Indeed, the utility of Kinect in medical applications, such as automated hip joint mobility assessment, has been well-demonstrated [22]. Beyond controlled laboratory settings, the non-invasive and affordable nature of the Kinect sensor makes it a particularly compelling platform for longitudinal and real-world fatigue monitoring, where traditional motion capture infrastructure is neither practical nor scalable. This accessibility makes it an attractive tool for continuous monitoring outside of controlled laboratory environments.

Predicting and identifying human walking fatigue, especially the continuous trajectory of fatigue progression, presents a significant challenge. While deep learning (DL) approaches have shown remarkable success in various domains, their application in biomechanical studies, particularly those involving human movement and physiological states, is often hampered by the inherent scarcity of large, diverse datasets [23–25]. Training robust deep learning models typically requires vast amounts of labeled data, which are difficult and expensive to acquire in clinical or sports science settings. Consequently, models trained on limited datasets are prone to overfitting and may lack generalizability to new, unseen individuals [26–28]. This data bottleneck is especially pronounced in fatigue research, where collecting sufficiently long and physiologically meaningful walking trials from a large cohort is both time-consuming and physically demanding for participants. This limitation necessitates the exploration of data-efficient methodologies that can leverage smaller datasets effectively.

Optimization algorithms, such as the Grey Wolf Optimizer (GWO), have proven to be highly effective in identifying optimal parameters in complex systems across diverse fields, ranging from engineering design to energy systems [29]. The robustness and efficiency of GWO in converging to optimal solutions make it a compelling candidate for extracting meaningful features and coefficients from biomechanical data [30–33]. Its ability to navigate high-dimensional search spaces without requiring large training corpora positions GWO as a particularly suitable tool for the data-constrained domain of human fatigue modeling.

Our previous work laid the foundation for this study by identifying an interpretable eight-feature Kinect model capable of reproducing physiologically anchored walking-fatigue trajectories with high fidelity [34].

This discovery study utilized GWO to identify the optimum stride Kinect-features that best reconstruct a physiologically validated fatigue trajectory, demonstrating the power of GWO in

robust high-dimensional discovery and stable feature ranking. However, that work — like the broader literature — remained confined to characterizing fatigue within already-observed individuals, leaving a fundamental and clinically critical question unanswered: can the continuous fatigue trajectory of a previously unseen individual be reliably predicted without collecting a full trial from that person? This gap represents one of the most significant barriers to deploying fatigue monitoring systems in real-world settings, where it is neither practical nor safe to wait for a complete fatigue episode before providing an assessment. Building upon this foundation, the current study directly addresses this challenge by proposing a novel data-efficient framework that predicts the complete continuous walking fatigue trajectory of a new individual by leveraging a database of previously characterized fatigue profiles. Unlike deep learning approaches that demand large labeled datasets, or subject-specific models that offer no generalization, our approach transfers knowledge across individuals through alignment-based similarity search combined with GWO-anchored coefficient transfer strategies — namely Nearest Person, K-Nearest Neighbors (KNN), and a sophisticated Fuzzy Fusion method. This methodology not only overcomes the fundamental data scarcity limitation of existing approaches, but also introduces a principled and interpretable mechanism for cross-subject fatigue prediction that is grounded in physiologically meaningful features. The result is a practical, low-cost, and generalizable solution for continuous fatigue monitoring that brings objective real-world deployment meaningfully closer.

2. Methods

2.1. Overview of the Predictive Pipeline

This study introduces a novel pipeline designed to predict an individual's continuous walking-fatigue trajectory from a repository of previously discovered per-participant coefficient magnitudes and stride-level feature trajectories. The pipeline re-uses the feature extraction, Dynamic Time Warping (DTW)-based time normalization, and resampling procedures established in our discovery study [34]. The experimental protocol and equipment setup from that study — including the treadmill configuration, sensor placement, and stopping criteria — are summarized in Figure 1 for reference. The eight gait features extracted from the Kinect v2 skeleton data, along with their anatomical locations on the body, are illustrated in Figure 2.

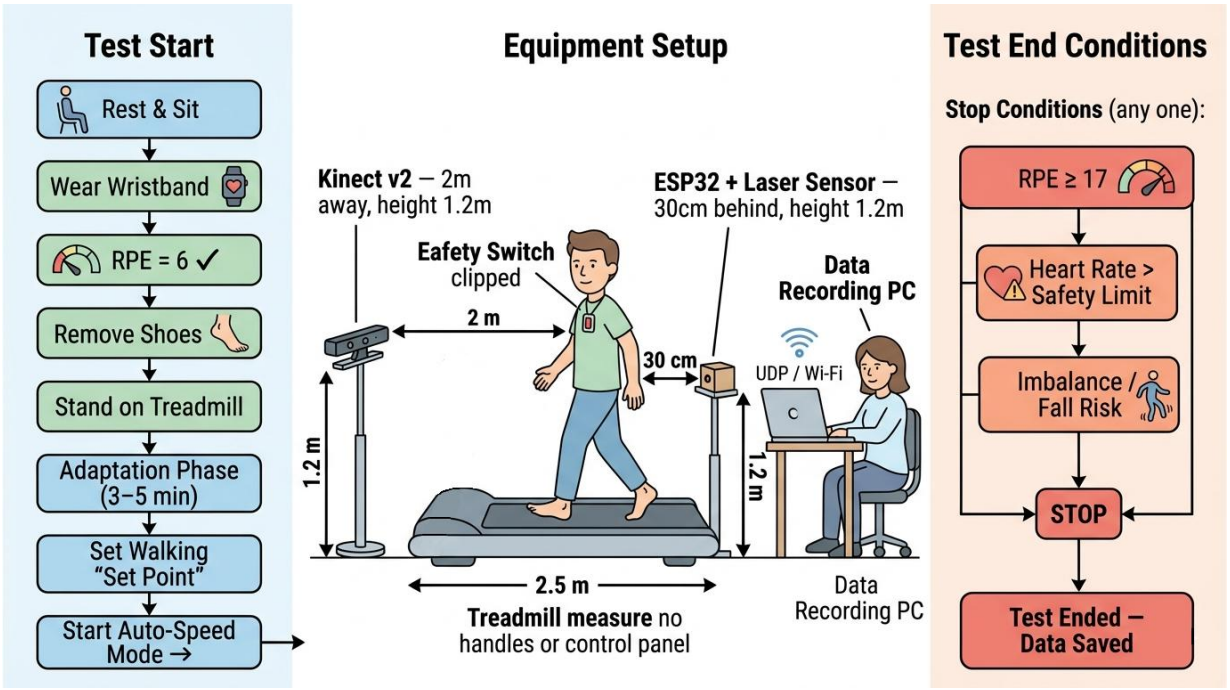


Fig. 1 Summary of the experimental protocol and equipment setup used in the discovery study. The center panel shows the treadmill and Kinect v2 sensor placement with key measurements. The left panel outlines the test initiation procedure and the right panel describes the conditions under which the test was terminated [34].

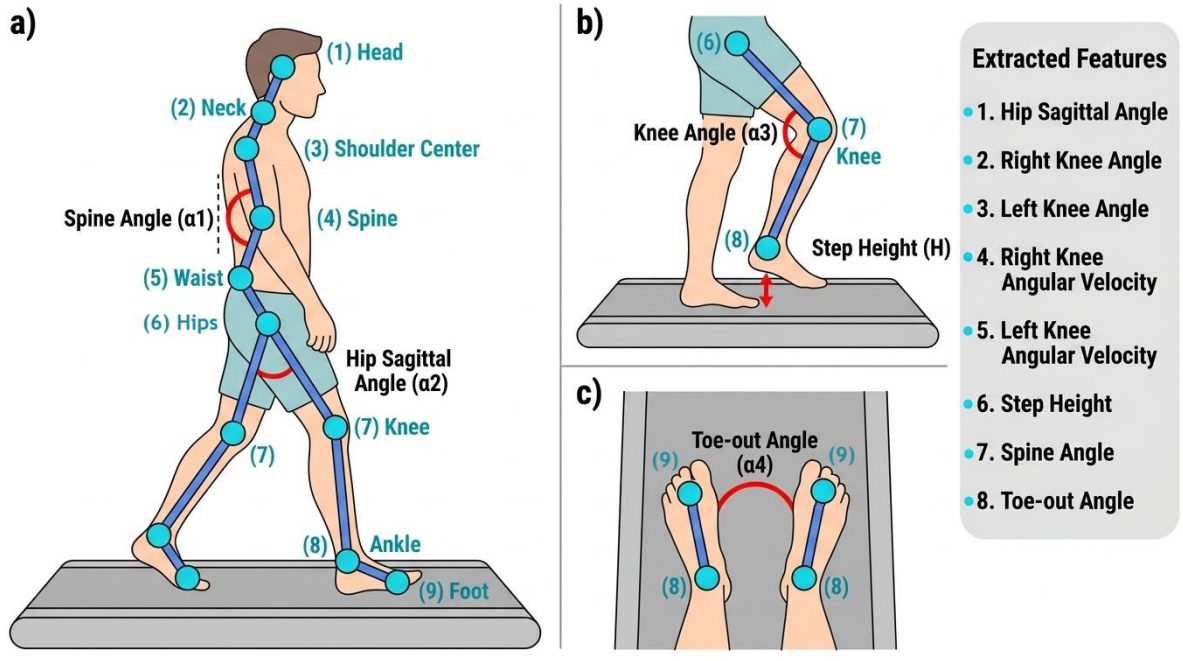


Fig. 2 Body joint landmarks detected by the Kinect v2 sensor and the eight gait features extracted for fatigue analysis: (a) spine angle (α1) and hip sagittal angle (α2) in the sagittal plane; (b) knee angle (α3) and step height (H) from a lateral close-up view; and (c) toe-out angle (α4) from a top-down perspective.

The pipeline then applies an alignment-based similarity search and a coefficient-transfer scheme, evaluated under a strict leave-one-subject-out (LOSO) protocol to ensure robust generalization.

2.2. Participants and Dataset

The predictive experiments utilized a pooled dataset comprising the original discovery cohort of 33 participants and newly recorded trials collected under the same protocol, resulting in a total of N=42 participants for final evaluation. The final cohort consisted of 42 healthy young adults (25 men, 17 women; age 19–23 years; mean age 20.57 ± 1.15 years; BMI 24.04 ± 3.79 $kg \cdot m^{-2}$, range 17.9–32.5 $kg \cdot m^{-2}$; BMI < 35 $kg \cdot m^{-2}$). All participants reported at least 20 min of daily walking and had no cardiovascular, metabolic, or musculoskeletal disease. All participants provided written informed consent, and the study received institutional ethics approval (**IR.SEMUMS.REC.1403.308**). Inclusion/exclusion criteria and demographics were consistent with the discovery study, focusing on healthy young adults, habitual walkers, with a BMI < 35 $kg \cdot m^{-2}$, and no cardiovascular, metabolic, or musculoskeletal diseases. A fixed-duration pilot set of 15 repeat recordings (200 seconds each) was also used to assess within- versus between-subject similarity, forming a 15 × 15 similarity matrix for initial validation.

2.3. Experimental Setup and Reference Fatigue Trajectory

Data acquisition and fatigue induction protocols mirrored those of the discovery study. Participants walked at a comfortable, self-selected pace on a treadmill while a Kinect v2 sensor recorded 3-D joint positions. Borg Ratings of Perceived Exertion (RPE) were recorded during each trial, serving as the empirical reference fatigue trajectory. All Borg RPE time series were aligned and time-normalized to a common 0–100% Fatigue Progression Time (FPT) using Dynamic Time Warping (DTW) prior to analysis, ensuring a standardized representation of fatigue progression.

2.4. Stride Features and Resampling

We employed the same eight stride-resolved Kinect-derived features identified as optimal in the discovery stage. These features include hip sagittal angle, right knee angle, left/right knee angular velocities, step height, spine angle, and toe-out. For each recording and each feature, stride-level values were linearly rescaled to a 0–100 range using the recording's dynamic range. Subsequently, these values were uniformly resampled (interpolated) to a common grid of $P=100$ points, representing 0–100% FPT. We denote the resampled trajectory of feature f for repository (database) recording r as $X_{r,f}(p)$ and for the query (held-out) recording as $X_{r,f}(p)$, where $p = 1, \dots, P$. Each repository recording r also provides previously discovered per-feature coefficient magnitudes $c_{r,f}$ (positive magnitudes retained from the discovery stage), which were optimized using the Grey Wolf Optimizer (GWO) as detailed in our prior work [34].

2.5. Normalization of Query Features Prior to Similarity Computation

Before computing similarity, each query feature trajectory was rescaled to match the dynamic range of the candidate repository record. This step ensures that comparisons are made on a common scale. Specifically, when comparing the query to repository record r, each $X_{q,f}$ was linearly rescaled using the stored minimum and maximum values of $X_{r,f}$, such that the rescaled query occupies the same 0–100 range as $X_{r,f}$. This normalization is crucial for accurate alignment and similarity assessment.

2.6. Alignment-Based Similarity

To account for potential temporal offsets between trials, similarity was computed by aligning the *P*-length query vector within each repository trajectory and evaluating the squared alignment error. For a repository record *r*, feature *f*, and an integer shift *s* (ensuring the aligned window remains valid), the shifted mean-squared error (MSE) is defined as:

$$\mathrm{MSE}_{r,f}(s) = \frac{1}{P}\sum_{p=1}^{P}[X_{r,f}(p+s) - X_{q,f}(p)]^2 \quad (1)$$

where shifts *s* that would place indices outside the repository trajectory are treated as out-of-bound. Each shifted MSE is then converted to an alignment-level similarity by inversion:

$$\mathrm{AlignmentSim}_{r,f}(s) = \begin{cases} BoundaryValue\ , \text{if shift } s\ is \text{ out of bound} \\ \dfrac{SIM_SCALE}{MSE_{r,f}(s)}\ , \text{otherwise} \end{cases} \quad (2)$$

2.7. Aggregation Across Features and Selection of Best Alignment

To aggregate feature-wise alignment errors into a single shift-level value for repository record *r*, the stored GWO-optimized coefficient magnitudes $c_{r,f}$ were used as feature importance weights. For each shift *s*, the weighted MSE was computed as:

$$\mathrm{WeightedMSE}_r(s) = \frac{\sum_{f=1}^{8} c_{r,f}\,\mathrm{MSE}_{r,f}(s)}{\sum_{f=1}^{8} c_{r,f}} \quad (3)$$

The corresponding combined alignment similarity is then:

$$\mathrm{CombinedSim}_r(s) = \frac{\mathrm{SIM_SCALE}}{\mathrm{WeightedMSE}_r(s)} \quad (4)$$

A single scalar participant similarity index for repository record *r* is obtained by selecting the best alignment, which corresponds to the maximum combined similarity across all valid shifts:

$$\mathrm{SimIndex}_r = \max_{s\in\mathcal{S}_r}\ \mathrm{CombinedSim}_r(s) \quad (5)$$

These $\mathrm{SimIndex}_r$ values are subsequently used to rank repository records for coefficient transfer strategies.

2.8. Coefficient-Transfer Strategies

Given the participant similarity indices $\mathrm{SimIndex}_r$ for all repository records, coefficient magnitudes for the query participant are estimated using three distinct strategies:

2.8.1. Nearest-Person (K=1)

This strategy selects the repository record r^* with the highest similarity index and directly assigns its stored coefficient magnitudes to the query participant:

$$\widehat{w}_f = c_{r^*,f} \tag{6}$$

2.8.2. K-Nearest Neighbors (KNN)

For KNN, the top-*K* repository records, ordered by SimIndex_r $(r_1, \ldots, r_K)$, are selected. The query coefficient magnitudes are then computed as a similarity-weighted average of their stored magnitudes:

$$\widehat{w}_f = \frac{\sum_{j=1}^{K} \text{SimIndex}_{r_j} \, c_{r_j,f}}{\sum_{j=1}^{K} \text{SimIndex}_{r_j}} \tag{7}$$

This study evaluated KNN for *K* values ranging from 2 to 9.

2.8.3. Fuzzy Fusion (Database-Wide Fuzzy Weighting)

This advanced method applies across the entire repository, not limited to a local neighborhood. Each participant similarity index SimIndex_r is mapped to a fuzzy membership scalar m_r via a three-band Gaussian Mamdani mapping. This mapping uses centers {20, 50, 80}, a spread $\sigma = 15$, and singleton outputs {0.1, 0.5, 1.0}. Specifically, for each repository record *r*, Gaussian membership functions are computed:

$$\mu_{\text{Low}}(r) = \exp\left(-\frac{(\text{SimIndex}_r - 20)^2}{2\sigma^2}\right) \tag{8}$$

$$\mu_{\text{Med}}(r) = \exp\left(-\frac{(\text{SimIndex}_r - 50)^2}{2\sigma^2}\right) \tag{9}$$

$$\mu_{\text{High}}(r) = \exp\left(-\frac{(\text{SimIndex}_r - 80)^2}{2\sigma^2}\right) \tag{10}$$

These are then defuzzified to obtain m_r:

$$m_r = \frac{\mu_{\text{Low}}(r) \cdot 0.1 + \mu_{\text{Med}}(r) \cdot 0.5 + \mu_{\text{High}}(r) \cdot 1.0}{\mu_{\text{Low}}(r) + \mu_{\text{Med}}(r) + \mu_{\text{High}}(r)} \tag{11}$$

Fuzzy fusion then produces the estimated coefficients by weighting all repository coefficient vectors by m_r:

$$\widehat{w}_f = \frac{\sum_r m_r \, c_{r,f}}{\sum_r m_r} \tag{12}$$

This approach generates a smoothly blended coefficient vector that reflects the continuous similarity structure of the entire database, contributing to enhanced robustness and generalization.

2.9. Reconstruction of Predicted Fatigue Trajectory

Given the fused coefficients $\widehat{w}_f$ *and the query participant's normalized features* $X_{q,f}(p)$, the predicted continuous fatigue trajectory on the p grid is reconstructed as a weighted sum of the features:

$$\hat{F}(p) = \sum_{f=1}^{8} \widehat{w}_f \, X_{q,f}(p) \ , \qquad p = 1, \dots, P. \tag{13}$$

Per-feature contribution traces $\widehat{w}_f \, X_{q,f}(p)$ were retained for visualization and interpretability.

2.10. Evaluation Protocol and Metrics

Predictive performance was rigorously assessed under a strict Leave-One-Subject-Out (LOSO) testing protocol. For each held-out recording (the query):

1. The query participant was excluded from the repository.
2. Query features were normalized to each candidate repository record's dynamic range.
3. $\mathrm{SimIndex}_r$ was computed for all remaining records using the entire held-out time series.
4. Fused coefficients were derived using each transfer strategy (Nearest, KNN with K *in {1-9}*, and Fuzzy).
5. The reconstructed fatigue trajectory $\hat{F}(p)$ was compared to the DTW-normalized Borg reference $F_{\mathrm{Borg}}(p)$.

The primary error metric used was the Euclidean distance between the predicted and actual fatigue curves, normalized by dividing by 100. This metric quantifies the average deviation of the predicted curve from the ground truth, with lower values indicating better performance. For clarity and intuitive interpretation in the results section, this error will also be presented as a Fidelity Score (100 - Error), where higher values indicate greater accuracy in reconstructing the fatigue trajectory.

2.11. External Validation

To further assess the generalizability and robustness of the proposed methods, an external validation was performed using data from three additional participants who were not part of the original 38-participant database. For each of these new participants, their fatigue curves were reconstructed using the Nearest Person, KNN (with $K=7$ as the best-performing KNN variant from the LOSO analysis), and Fuzzy Fusion methods. The predicted curves were then compared against their actual fatigue trajectories using the same error metric described in Section 2.10. This independent validation provides crucial evidence of the model's performance on unseen data, simulating real-world application scenarios.

3. Results

3.1. Validation of 200-Second Gait Signature for Participant Identification

To ascertain the efficacy of a short, 200-second walking trial in identifying individual gait-fatigue signatures, a 15 × 15 similarity matrix was generated by comparing 200-second test runs against full fatigue runs from a database of 15 participants. The analysis revealed a clear and statistically significant distinction between self-similarity (a participant matching their own record) and cross-similarity (a participant matching another's record).

As summarized in Table 1, the mean self-similarity was 96.88% (SD = 1.63%), while the mean cross-similarity was substantially lower at 83.33% (SD = 5.72%). Notably, the lowest self-similarity observed (93.76%) remained higher than the highest cross-similarity (88.84%), indicating no overlap between the two distributions. A Welch's t-test confirmed an extremely significant difference between self-similarity and cross-similarity ($t = 23.01$, $p < 0.0001$). Furthermore, the calculated Cohen's d of 3.22 signifies an exceptionally large effect size, underscoring the strong discriminative power of the 200-second gait signature. Crucially, the identification accuracy was 100%, meaning that for every participant, their 200-second test run yielded the highest similarity score with their own full fatigue run in the database.

Table 1 Statistical Comparison of Self-Similarity vs. Cross-Similarity from 200-Second Gait Signatures.

Metric	Self-Similarity (N=15)	Cross-Similarity (N=210)	Statistical Test (Welch's t-test)
Mean (%)	96.88	83.33	$t = 23.01, p < 0.0001$
Standard Deviation (%)	1.63	5.72	Cohen's $d = 3.22$
Median (%)	97.46	86.96	
Min (%)	93.76	60.78	
Max (%)	98.96	88.84	
Identification Accuracy	100%	N/A	

These results unequivocally demonstrate that a 200-second walking trial is sufficient to reliably identify individuals within the database based on their unique gait-fatigue features, providing a robust foundation for the subsequent coefficient transfer process.

3.2. Leave-One-Subject-Out (LOSO) Cross-Validation of Fatigue Curve Reconstruction

The performance of the three coefficient-transfer strategies (Nearest Person, KNN with varying K, and Fuzzy Fusion) was rigorously evaluated using a Leave-One-Subject-Out (LOSO) cross-

validation protocol across 38 participants. The primary metric, Mean Absolute Error (MAE), was derived from the Euclidean distance between the predicted and actual DTW-normalized fatigue curves, divided by 100. For enhanced interpretability, we also present a Fidelity Score (100 - MAE), where higher values indicate better reconstruction accuracy.

Table 2 Performance of Coefficient Transfer Strategies in LOSO Cross-Validation (N=38).

Method	Mean MAE (%)	Fidelity Score (100-MAE) (%)	SD (MAE)	Median (MAE)	RMSE (MAE)	Acc ≤ 10% (MAE)	Acc ≤ 5% (MAE)
Nearest Person	13.95	86.05	4.49	14.25	14.64	18.42%	0.00%
KNN (K=2)	13.16	86.84	3.97	13.23	13.73	23.68%	0.00%
KNN (K=3)	13.45	86.55	4.93	12.94	14.31	18.42%	0.00%
KNN (K=4)	13.45	86.55	4.52	13.48	14.17	21.05%	0.00%
KNN (K=5)	13.75	86.25	4.68	13.97	14.50	21.05%	0.00%
KNN (K=6)	13.46	86.54	4.38	13.85	14.13	21.05%	2.63%
KNN (K=7)	**12.94**	**87.06**	**3.76**	**13.26**	**13.46**	**23.68%**	**0.00%**
KNN (K=8)	13.37	86.63	4.14	13.43	13.98	21.05%	0.00%
KNN (K=9)	13.49	86.51	4.03	13.81	14.06	21.05%	0.00%
Fuzzy Fusion	**9.12**	**90.88**	**2.70**	**9.07**	**9.50**	**71.05%**	**5.26%**

As presented in Table 2, the Fuzzy Fusion method consistently demonstrated superior performance across all metrics. It achieved the lowest Mean MAE of 9.12% (corresponding to a Fidelity Score of 90.88%), significantly outperforming the Nearest Person method (MAE = 13.95%) and the best-performing KNN variant (K=7, MAE = 12.94%).

The standard deviation of MAE for Fuzzy Fusion (2.70%) was also considerably lower, indicating greater consistency and robustness across participants. For better visualasion all participants errors are bring as heatmap error in Figure 3.

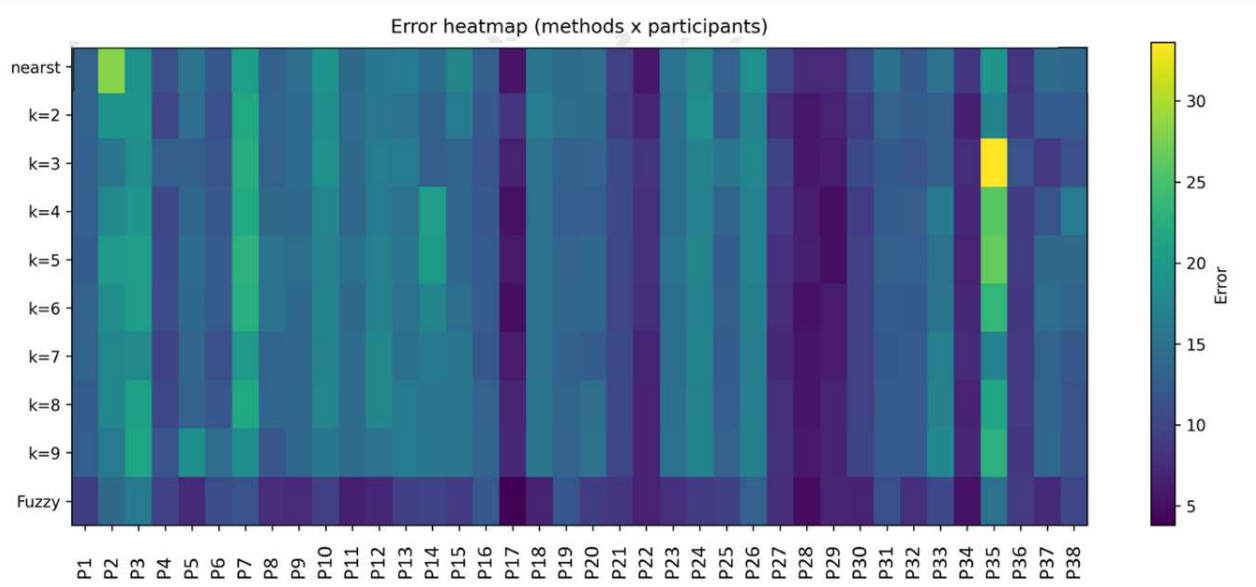


Fig. 3 Heatmap of Reconstruction Fidelity across the Participant Database.The heatmap illustrates the error distribution for all 38 participants under the Leave-One-Subject-Out (LOSO) protocol.

Furthermore, Fuzzy Fusion achieved an impressive 71.05% of predictions with an MAE of 10% or less, and 5.26% with an MAE of 5% or less. In contrast, the best KNN method (K=7) only achieved 23.68% for MAE ≤ 10% and 0% for MAE ≤ 5%This highlights the enhanced precision of the Fuzzy approach.

Comparative analysis using Cohen's *d* revealed large to very large effect sizes when comparing Fuzzy Fusion to other methods. For instance, the Cohen's *d* for Fuzzy vs. Nearest Person was 1.47, and for Fuzzy vs. KNN (K=7) was 1.25. These substantial effect sizes underscore the practical significance of the performance gains achieved by Fuzzy Fusion.

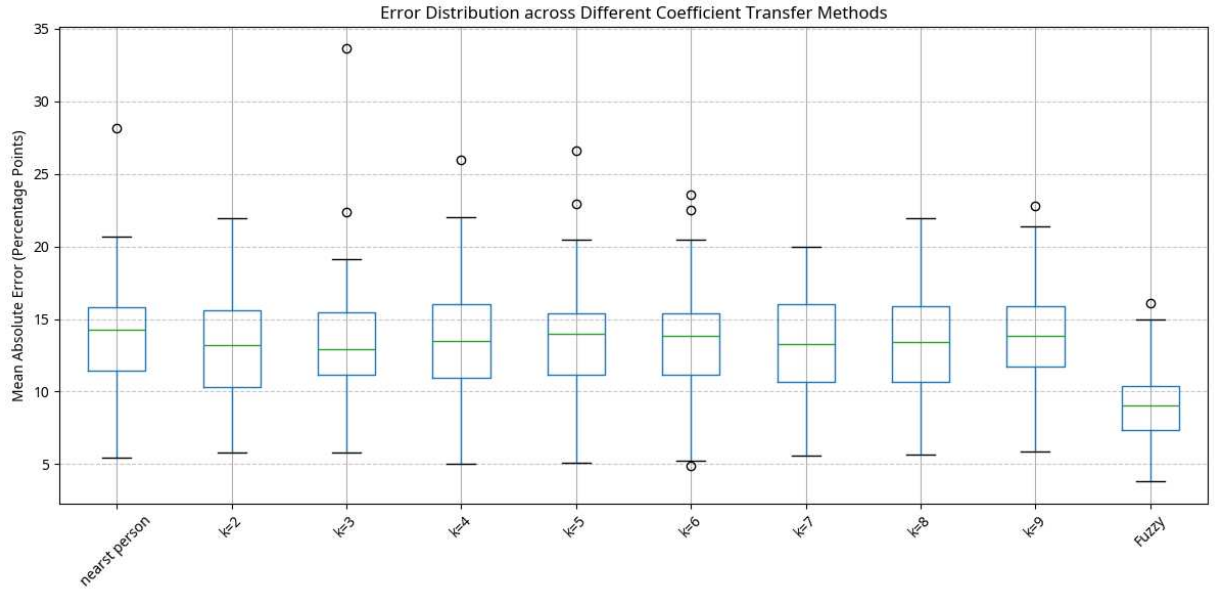


Fig. 4 Boxplot of Error Distribution across Different Coefficient Transfer Methods in LOSO Cross-Validation.

Figure 4 visually corroborates these findings, illustrating that the error distribution for Fuzzy Fusion is not only centered at a lower value but also exhibits a significantly narrower interquartile range and fewer outliers compared to all other methods. This graphical

representation clearly identifies Fuzzy Fusion as the most accurate and robust strategy for reconstructing individual fatigue trajectories.

3.3. External Validation on Unseen Participants

To further validate the generalizability of the proposed methodology, three participants not included in the original database were subjected to the same prediction pipeline. Their fatigue curves were reconstructed using the Nearest Person, KNN (K=7), and Fuzzy Fusion methods, and the MAE was calculated against their actual fatigue trajectories. The results, summarized in Table 3, provide compelling evidence of the model's performance on truly unseen data.

Table 3 Performance of Coefficient Transfer Strategies on External Validation (N=3 Unseen Participants).

Method	Mean MAE (%)	Fidelity Score (100-MAE) (%)	Individual MAE (%)
Nearest Person	20.87	79.13	14.20, 30.05, 18.35
KNN (K=7)	19.33	80.67	13.37, 27.01, 17.61
Fuzzy Fusion	**10.61**	**89.39**	**9.26, 10.97, 11.60**

For these three unseen participants, Fuzzy Fusion achieved a mean MAE of 10.61% (Fidelity Score = 89.39%), demonstrating a substantial improvement over both Nearest Person (Mean MAE = 20.87%) and KNN (K=7, Mean MAE = 19.33%). Specifically, Fuzzy Fusion reduced the mean error by 49.15% compared to the Nearest Person method and by 45.11% compared to the best KNN (K=7). Furthermore, the individual MAE values for Fuzzy Fusion were remarkably consistent (ranging from 9.26% to 11.60%), especially when contrasted with the wide variability observed in the Nearest Person method (14.20% to 30.05%). This stability in prediction for unseen individuals highlights the superior robustness and generalizability of the Fuzzy Fusion approach.

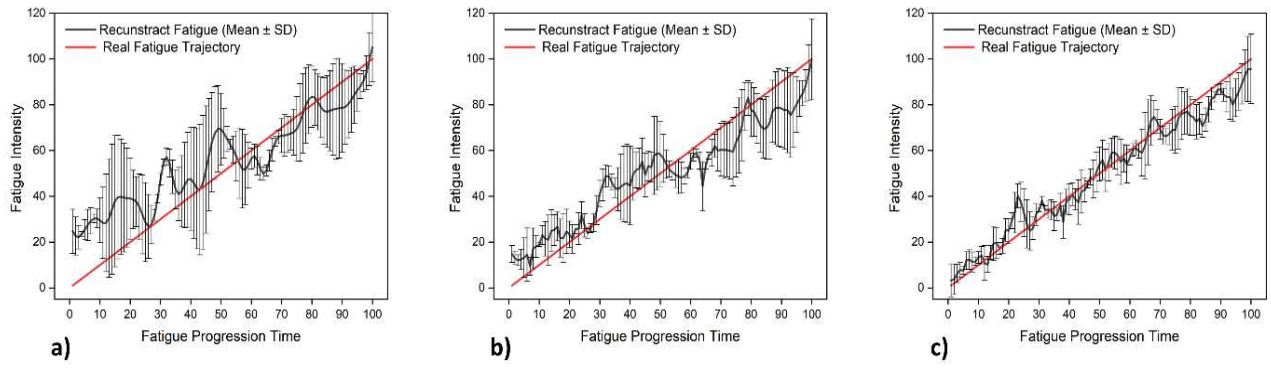


Fig. 5 Reconstructed Fatigue Curves for an Unseen Participant using Nearest Person (a), KNN (K=7) (b), and Fuzzy (c) Fusion methods compared to the Actual Fatigue Curve.

4. Discussion

This study presents a novel and data-efficient approach for the continuous prediction of human walking fatigue trajectories, addressing a critical gap in low-cost, unobtrusive physiological monitoring. By leveraging an existing database of GWO-optimized fatigue coefficients and employing advanced similarity-based transfer learning strategies, we have demonstrated a robust method for estimating individual fatigue progression without the need for extensive subject-specific calibration or large datasets typically required by deep learning models.

The initial validation of the 200-second gait signature proved to be a cornerstone of our methodology. The ability to unequivocally identify individuals based on a short walking trial, as evidenced by 100% identification accuracy and an exceptionally large Cohen's *d* of 3.22, is highly significant. This finding suggests that each individual possesses a unique and consistent gait-fatigue signature that can be reliably captured within a brief observation period. This has profound implications for real-world applications, as it enables the system to rapidly identify a new user and access their most relevant fatigue profile from the database, thereby facilitating near real-time fatigue monitoring. This data-efficient identification mechanism circumvents the need for lengthy baseline measurements or complex model training for each new individual, which is a major advantage in practical settings.

The rigorous Leave-One-Subject-Out (LOSO) cross-validation provided compelling evidence for the superiority of the Fuzzy Fusion method. With a mean MAE of 9.12% (Fidelity Score of 90.88%), Fuzzy Fusion significantly outperformed both Nearest Person and all KNN variants. The substantial reduction in error, coupled with a lower standard deviation, highlights the enhanced accuracy and consistency of the fuzzy approach. The large effect sizes (Cohen's *d* up to 1.47) further underscore the practical significance of these improvements. This superior performance can be attributed to the inherent design of Fuzzy Fusion, which intelligently blends information from the entire database based on continuous similarity memberships. Unlike discrete methods like Nearest Person or KNN, which rely on a limited number of 'hard' neighbors, Fuzzy Fusion creates a smoothly weighted average of coefficients. This allows it to better account for the continuous spectrum of inter-individual variability in fatigue responses, leading to more generalized and robust predictions, especially when an exact match for a new individual is not present in the database [35, 36].

The external validation on three unseen participants further solidified the generalizability and real-world applicability of our Fuzzy Fusion model. The consistent and low MAE (mean 10.61%) for these independent subjects, along with the remarkable stability of predictions, demonstrates that the model is not merely overfitting to the training database but can effectively generalize to new individuals. The significant percentage reduction in error (up to 49.15% over Nearest Person) for these unseen cases provides strong evidence that this approach can be reliably deployed in diverse populations, even when their specific fatigue patterns are not explicitly stored in the database. This is a crucial aspect for any technology aiming for widespread adoption in clinical or sports monitoring.

The choice of GWO-optimized coefficients, derived from our previous work [34], is central to the physiological grounding of this predictive model. By anchoring the fatigue trajectory reconstruction to physiologically validated measures like Borg RPE and sEMG, the model ensures that the predicted fatigue is not merely a kinematic correlation but reflects actual physiological changes [37–39]. The stability and robustness of GWO in identifying these coefficients, as noted in our earlier discussions, further contribute to the reliability of the transferred knowledge. This approach stands in contrast to purely data-driven methods that might identify statistical correlations without a clear physiological basis, making the results

more interpretable and clinically relevant [40–42]. The successful application of GWO in other complex optimization problems, such as solar cell efficiency [29], further attests to its capability in extracting meaningful parameters from intricate systems.

This study effectively addresses the challenge of data scarcity in biomechanical research, particularly for continuous fatigue monitoring. While deep learning models often struggle with limited datasets, leading to overfitting and poor generalization [43, 44], our similarity-based transfer learning approach provides a viable alternative. By leveraging a well-characterized database and intelligently transferring GWO-optimized coefficients, we have developed a system that is both data-efficient and highly accurate. This methodology opens new avenues for personalized fatigue assessment, where a brief initial assessment can unlock a personalized predictive model based on a repository of similar individuals. This paradigm shift can accelerate the development of practical, low-cost, and continuous fatigue monitoring solutions, ultimately enhancing safety, performance, and well-being in various domains.

5. Conclusion

This study successfully developed and validated a novel data-efficient methodology for the continuous prediction of human walking fatigue trajectories. By integrating a robust 200-second gait signature for individual identification with GWO-anchored feature coefficients and an innovative Fuzzy Fusion transfer learning strategy, we have established a highly accurate and generalizable system. The Fuzzy Fusion method demonstrated clear superiority over traditional Nearest Person and KNN approaches, achieving a mean Fidelity Score of 90.88% in internal cross-validation and maintaining a high Fidelity Score of 89.39% when tested on entirely unseen participants.

These results signify a major advancement in addressing the "data bottleneck" in biomechanics. While deep learning models often require thousands of samples to generalize, our framework achieves high-fidelity reconstruction using a modest repository of physiologically grounded profiles. The use of the Fidelity Score as a performance metric underscores the model's ability to capture the nuanced, non-linear progression of fatigue with over 90% accuracy in most cases. This approach provides a practical, low-cost solution for real-time monitoring, enabling proactive interventions in rehabilitation and sports science. Future work will focus on expanding the database to include pathological gait patterns, further enhancing the clinical utility of this high-fidelity monitoring system.

Acknowledgement:

We appreciate the Department of Electrical and Computer Science at Semnan University for providing us with the necessary facilities and equipment for conducting our experiments.

Declarations

Competing interests:

The authors declare that they have no conflict of interest. This research was conducted in the absence of any commercial or financial relationships that could be construed as a potential conflict of interest.

Author contributions

The study conception and design were developed by Parham Yazdani, in consultation with Hadi Soltanizadeh. Material preparation, data collection, and analysis were performed by Parham Yazdani, with methodological guidance and algorithm selection provided by Hadi Soltanizadeh. Clinical interpretation and validation of the medical relevance of the findings were provided by Farhad Azadi and Mohammad Zahraei. The first draft of the manuscript was written by Parham Yazdani, and all authors commented on previous versions of the manuscript. All authors read and approved the final manuscript.

Ethics approval:

This study was approved by The Semnan University of Medical Sciences ethics committee (IR.SEMUMS.REC.1403.308).

Consent to participate:

All participants gave informed consent to participate in the study. The participants did not consent to have their data publicly available due to privacy and security concerns. The data are available from the corresponding author upon reasonable request and with the permission of the participants.

Consent to publish

Not applicable. This manuscript does not contain any individual person's data in any form (including images, videos, or identifiable case details). All figures presented are schematic illustrations or computer-generated graphics and do not depict any human research participant.

Data availability:

The data that support the findings of this study is available from the corresponding author upon reasonable request. The data are not publicly available due to their large size and the technical challenges of hosting and transferring them.

Material availability:

The materials that support the findings of this study are available from the corresponding author upon reasonable request. The materials are not publicly available due to their proprietary nature and the costs involved in acquiring them.

Code availability:

The code that supports the findings of this study are available from the corresponding author upon reasonable request. The codes are not publicly available due to their proprietary nature and the intellectual property rights involved.

References

1. Kao P-C, Lomasney C, Gu Y, et al (2023) Effects of induced motor fatigue on walking mechanics and energetics. J Biomech 156:111688

2. Wang L, Ma W, Zhu W, et al (2025) Effects of experimentally induced lower limb muscle fatigue on healthy adults' gait: a systematic review. Bioengineering 12:225
3. Jirsaraei MJ, Ji W, Acuña SA (2026) Kinematic indicators of physical fatigue during walking: A systematic review of assessment parameters and protocols. Appl Ergon 131:104640
4. Lin H, Wang H, Ke Y (2025) Research on optimization and improvement of sports fatigue training based on biomechanical principles. Molecular & Cellular Biomechanics 22:
5. Ahn CR, Lee S, Sun C, et al (2019) Wearable sensing technology applications in construction safety and health. J Constr Eng Manag 145:03119007
6. Li A (2025) Real-time athlete fatigue monitoring using fuzzy decision support systems. International Journal of Computational Intelligence Systems 18:23
7. Rudroff T (2025) Digital biomarkers and AI for remote monitoring of fatigue progression in neurological disorders: bridging mechanisms to clinical applications. Brain Sci 15:533
8. Borg GA V (1982) Psychophysical bases of perceived exertion. Med Sci Sports Exerc 14:377–381
9. Micklewright D, St Clair Gibson A, Gladwell V, Al Salman A (2017) Development and validity of the rating-of-fatigue scale. Sports Medicine 47:2375–2393
10. Borg E, Kaijser L (2006) A comparison between three rating scales for perceived exertion and two different work tests. Scand J Med Sci Sports 16:57–69
11. Völker I, Kirchner C, Bock OL (2016) On the relationship between subjective and objective measures of fatigue. Ergonomics 59:1259–1263
12. Chang K-M, Liu S-H, Wu X-H (2012) A wireless sEMG recording system and its application to muscle fatigue detection. Sensors 12:489–499
13. Lung C-W, Liau B-Y, Peters JA, et al (2021) Effects of various walking intensities on leg muscle fatigue and plantar pressure distributions. BMC Musculoskelet Disord 22:831
14. Zhang W, Bai Z, Yan P, et al (2024) Recognition of human lower limb motion and muscle fatigue status using a wearable FES-sEMG system. Sensors 24:2377
15. Byeon H, Seno ME, Yajid MSA, et al (2024) Wearable sensor technology and medical robotics for fatigue assessment using electromyography signal processing. Signal Image Video Process 18:8767–8780
16. Jirsaraei MJ, Ji W, Acuña SA (2026) Kinematic indicators of physical fatigue during walking: A systematic review of assessment parameters and protocols. Appl Ergon 131:104640
17. Pinto-Bernal MJ, Cifuentes CA, Perdomo O, et al (2021) A data-driven approach to physical fatigue management using wearable sensors to classify four diagnostic fatigue states. Sensors 21:6401
18. Baghdadi A, Cavuoto LA, Jones-Farmer A, et al (2021) Monitoring worker fatigue using wearable devices: A case study to detect changes in gait parameters. Journal of quality technology 53:47–71
19. Scataglini S, Abts E, Van Bocxlaer C, et al (2024) Accuracy, validity, and reliability of markerless camera-based 3D motion capture systems versus marker-based 3D motion capture systems in gait analysis: a systematic review and meta-analysis. Sensors 24:3686
20. Yamada T, Kondo K (2025) Non-Contact Fatigue Estimation in Healthy Individuals Using Azure Kinect: Contribution of Multiple Kinematic Features. Sensors 25:6633

21. Yazdani P, Soltanizadeh H, Zahraei M (2026) Automated hip joint mobility assessment using fuzzy algorithms, kinect sensor and clinical expertise. Research on Biomedical Engineering 42:6
22. Yazdani P, Soltanizadeh H, Zahraei M (2026) Automated hip joint mobility assessment using fuzzy algorithms, kinect sensor and clinical expertise. Research on Biomedical Engineering 42:6
23. Friemert D, Schnur D, Runkel S, et al (2025) Limitations of Public Biomechanical Movement Datasets for Deep Learning: Issues of Metadata, Standardization, and Variety in Motion Types. medRxiv 2025
24. Prakash C, Kumar R, Mittal N (2018) Recent developments in human gait research: parameters, approaches, applications, machine learning techniques, datasets and challenges. Artif Intell Rev 49:1–40
25. Bicer M, Phillips ATM, Melis A, et al (2022) Generative deep learning applied to biomechanics: A new augmentation technique for motion capture datasets. J Biomech 144:111301
26. Liew BXW, Pfisterer F, Rügamer D, Zhai X (2024) Strategies to optimise machine learning classification performance when using biomechanical features. J Biomech 165:111998
27. Dindorf C, Dully J, Konradi J, et al (2024) Enhancing biomechanical machine learning with limited data: generating realistic synthetic posture data using generative artificial intelligence. Front Bioeng Biotechnol 12:1350135
28. Halmich C, Höschler L, Schranz C, Borgelt C (2025) Data augmentation of time-series data in human movement biomechanics: A scoping review. PLoS One 20:e0327038
29. Yazdani P, Orouji AA, Gharibshahian I, Soltanizadeh H (2024) Achieving an efficient Sb2Se3-based solar cell by improving the performance parameters using the grey wolf optimization algorithm. Solar Energy Materials and Solar Cells 269:112796
30. Wang X, Li Z, Kang H, et al (2021) Medical image segmentation using PCNN based on multi-feature grey wolf optimizer bionic algorithm. J Bionic Eng 18:711–720
31. Mafarja M, Thaher T, Too J, et al (2023) An efficient high-dimensional feature selection approach driven by enhanced multi-strategy grey wolf optimizer for biological data classification. Neural Comput Appl 35:1749–1775
32. Sallam NM, Saleh AI, Arafat Ali H, Abdelsalam MM (2022) An efficient strategy for blood diseases detection based on grey wolf optimization as feature selection and machine learning techniques. Applied Sciences 12:10760
33. Chakraborty C, Kishor A, Rodrigues JJPC (2022) Novel enhanced-grey wolf optimization hybrid machine learning technique for biomedical data computation. Computers and Electrical Engineering 99:107778
34. Yazdani P, Soltanizadeh H, Maleki A, et al (2026) Evaluation of Fatigue Intensity from Gait Data: A Mathematical Model. Proceedings of the National Academy of Sciences, India Section A: Physical Sciences 1–18
35. Basheer S, Nagwanshi KK, Bhatia S, et al (2021) FESD: An approach for biometric human footprint matching using fuzzy ensemble learning. Ieee Access 9:26641–26663
36. Al-Kasasbeh RT, Korenevskiy NA, Aikeyeva AA, et al (2020) Developing a biotech scheme using fuzzy logic model to predict occurrence of diseases using person's functional state. International Journal of Computer Applications in Technology 62:257–267
37. Troiano A, Naddeo F, Sosso E, et al (2008) Assessment of force and fatigue in isometric contractions of the upper trapezius muscle by surface EMG signal and perceived exertion scale. Gait Posture 28:179–186

38. Zhou Q, Chen Y, Ma C, Zheng X (2011) Evaluation of upper limb muscle fatigue based on surface electromyography. Sci China Life Sci 54:939–944
39. Cerqueira SM, Vilas Boas R, Figueiredo J, Santos CP (2024) A comprehensive dataset of surface electromyography and self-perceived fatigue levels for muscle fatigue analysis. Sensors 24:8081
40. Oakden-Rayner L, Carneiro G, Bessen T, et al (2017) Precision radiology: predicting longevity using feature engineering and deep learning methods in a radiomics framework. Sci Rep 7:1648
41. Tanasković I, Lazarević LB, Knežević G, et al (2025) Interpretable machine learning for cardiogram-based biometrics. arXiv preprint arXiv:251019775
42. Bento N, Rebelo J, Barandas M, et al (2022) Comparing handcrafted features and deep neural representations for domain generalization in human activity recognition. Sensors 22:7324
43. Kanjilal R, Uysal I (2021) The future of human activity recognition: Deep learning or feature engineering? Neural Process Lett 53:561–579
44. Binson VA, Thomas S, Subramoniam M, et al (2024) A review of machine learning algorithms for biomedical applications. Ann Biomed Eng 52:1159–1183